Steel Structures Research Update

Seismic Performance and Design of Steel Panel Dampers for Steel Moment Frames

JUDY LIU

INTRODUCTION

Ongoing work on the seismic performance and design of steel panel dampers for steel moment frames is highlighted. Dr. Keh-Chyuan Tsai, professor in the Department of Civil Engineering at National Taiwan University, leads the team from National Taiwan University and the National Center for Research on Earthquake Engineering (NCREE) in Taipei. In 2018, Dr. Tsai received an AISC Special Achievement Award in recognition of "extensive work with U.S. researchers to conduct large-scale system level testing of structural steel seismic force resisting systems, leading to system level verification of many of the AISC 341 provisions" (AISC, 2018).

At NCREE, one recent collaboration with the University of Washington included cyclic tests of a three-story chevron special concentrically braced frame (SCBF). Current seismic design provisions require large beam sizes to resist the unbalanced forces from the chevron braces after brace buckling. The research has explored options for alternative ductile mechanisms and reduced beam sizes. The three-story tests followed a series of one-story frame tests, demonstrating that beam yielding following brace buckling "improved the deformability of the SCBF without compromising the capacity of the system," and highlighting limitations with respect to weak beams (NCREE, 2018). The three-story tests were used to validate finite element models and to further inform proposed design requirements for the AISC *Seismic Provisions*.

Steel research at NCREE has also included studies on steel beam-to-box-column moment connections and electro-slag-welded (ESW) joints in those connections. Cyclic tests on full-scale, welded beam-to-box-column connections showed inadequate strength and ductility as a result of diaphragm plates that had not been properly welded to the columns (Tsai et al., 2015). Tsai et al. (2015) developed recommendations for improved design, fabrication and inspection procedures. Meanwhile, research into premature fracture of ESW diaphragm-to-column joints in beam-to-box-column connections has revealed sensitivity to eccentricity in loading between the beam flange and the diaphragm. Further, a micromechanical-based stress-modified critical stress (SMCS) model has been developed and shown to be capable of predicting the crack initiation of the diaphragm-to-column ESW joint (Li et al., 2018).

Judy Liu, Ph.D., Research Editor of the AISC *Engineering Journal*, Professor, Oregon State University, School of Civil & Construction Engineering, Corvallis, OR. Email: judy.Liu@oregonstate.edu

The steel panel damper research described here complements a variety of studies around the world focused on providing supplemental energy dissipation for improved seismic performance. From Argentina, the multiple friction damper (MFD) is composed of friction elements that can be stacked around an existing column to dissipate energy with horizontal movement of the column (Martinez and Curadelli, 2017). In China, the curved surfaces of the arc-surfaced frictional damper (AFD) in a diagonal brace, for example, result in damping forces that vary with displacement (Wang et al., 2017). Korean researchers have combined a steel slit damper and rotational friction dampers for seismic retrofit of a reinforced concrete (RC) moment frame with core walls (Lee et al., 2017) and have also explored a set of steel slit dampers assembled into a box shape and used in knee braces for retrofit of an RC moment frame (Lee and Kim, 2017). The steel panel dampers utilize a different mechanism but share the common goal of reducing deformation and force demands on the system.

RESEARCH OBJECTIVES

Motivated in part by the 1995 Great Hanshin-Awaji earthquake, researchers have sought methods to improve the performance of seismic-force-resisting systems such as steel moment-resisting frames (MRFs). Among the methods explored were low-yield-stress steel shear panel dampers, shown by Liu et al. (2007), Otani et al. (2001), and Tanaka and Sasaki (2000) to provide good energy dissipation capacity. Contemporary work by Tsai et al. (2001) demonstrated through substructure pseudodynamic tests and analysis that low-yield steel shear panel dampers as additional Vierendeel frame "columns" improved performance by exhibiting "excellent energy dissipation characteristics thereby reducing the inelastic deformational demand imposed on the beam-to-column connections in the conventional MRFs."

Tsai et al. (2018) have developed the steel panel damper

(SPD) incorporated into a SPD-MRF as shown in Figure 1. The SPD features three segments: a middle inelastic core (IC) with buckling-restraining stiffeners and two elastic joint (EJ) segments top and bottom. The three segments are fabricated from two different I-sections, with the two EJ segments using the same, stronger section. All segments are rigidly connected to each other and to the boundary beams and remain elastic in a service level earthquake (SLE). The inelastic core (IC) is expected to see inelastic shear deformations in a design basis earthquake (DBE) or maximum considered earthquake (MCE) and to dissipate energy through significant inelastic shear deformations in a severe earthquake. Shear buckling at large deformations is prevented by the stiffeners.

Much of the SPD-related research to date has focused on the behavior, design and detailing of the inelastic core (IC), or shear panel (e.g., Chen et al., 2006). Information on the seismic performance of SPD-MRFs is lacking, as are comprehensive guidelines for seismic design of the three-segment SPDs and the SPD-MRF. The overarching goal of the research has been to fill the knowledge gaps, and Tsai et al. (2018) have accomplished this through testing of two full-scale SPD specimens and numerical simulations using Abaqus and PISA3D. Specifically, for SPD-MRF design and evaluation, research objectives are to provide procedures for design of the IC segment; to develop capacity design methods (CDM) for the EJ segments, boundary beams, and the SPD-to-beam panel zones; and to develop numerical models, including a three-segment SPD model and an equivalent one-element model.

SEISMIC DESIGN WITH STEEL PANEL DAMPERS

The performance objectives for the SPD and SPD-MRF include the requirement that all elements remain elastic in an SLE, that the inelastic shear deformations are concentrated in the inelastic core (IC) for a DBE or MCE, and that the SPD is able to dissipate energy through significant inelastic shear deformations in the MCE. SPD design and detailing requirements, including details of the buckling-restraining stiffeners in the IC, have been developed. Capacity design methods (CDM) for the elastic joints (EJ) and the boundary beams have also been developed.

Seismic Design of SPDs

The design of the SPD centers on the energy-dissipating IC, which has a thinner or weaker web than the EJ segments. The flanges of the SPD are considered to be continuous over the three segments. The strength of the SPD is governed by shear yielding of the IC, assuming axial load effects to be insignificant. The SPD stiffness can be adjusted by changing the relative heights of the two identical EJ and of the IC, as well as by stiffening the EJ.

Capacity design of the EJ is achieved by considering the shear and moment expected from full shear yielding of the IC. Shear demands on the EJ are calculated with the shear yield strength using the expected yield stress, R_yF_y, and a strain-hardening factor for the web of the IC. For calculation of the corresponding maximum EJ moment demands, an inflection point is assumed at mid-height of the SPD. Though the proposed approach does not consider shear-moment interaction, Tsai et al. (2018) also propose an alternative, more conservative approach with calculations of von Mises stresses.

The web and end stiffeners of the IC (Figure 1) delay the onset of shear buckling to maximize energy dissipation in the case of severe earthquakes. Design and detailing of the stiffeners follow the requirements developed by Chen et al. (2006). The end stiffeners are full depth, are welded to the SPD flanges, and form the boundaries between the IC and the EJ. The IC and EJ webs are welded to either side of an end stiffener. Vertical and horizontal web, or buckling-restraining, stiffeners can be welded to opposite sides of the web. These web stiffeners are also welded to the end stiffeners or SPD flanges, as applicable. Spacing of the IC

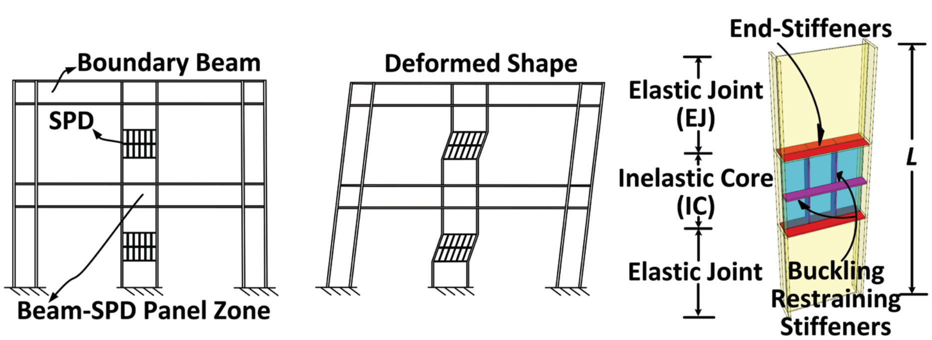

Fig. 1. Schematics of SPD and SPD-MRF.

web stiffeners is chosen to satisfy the recommended limits on slenderness of the web between stiffeners (Chen et al., 2006). All stiffeners are sized to delay out-of-plane buckling using a rigidity requirement developed by Chen et al. (2006). The end and horizontal web stiffeners are also sized for axial force demands from shear buckling and the development of tension field action in the IC web so as to "resist the pull-in forces" on the IC flanges (Tsai et al., 2018).

For calculations of SPD lateral stiffness in cases with no rotation at the boundary beams, Tsai et al. (2018) provide an equation that includes the shear and bending stiffnesses of the IC and EJ segments. The equation can be used for the SPD post-yield stiffness by modifying the shear modulus for the IC by a strain hardening ratio as adopted for a bilinear material stress-strain relationship.

Seismic Design of Steel MRFs with SPDs

Seismic design of SPD-MRF requires capacity design of the boundary beams and of the SPD-to-beam panel zones. As for ductile design of conventional MRF, inelastic behavior in the beams should be restricted to the ends, at the beam-to-column connections. Recommendations for capacity design of the boundary beams are based on seismic provisions to prevent shear or flexural yielding in the beam outside the link in eccentrically braced frames (AISC, 2016). Similarly, the SPD-to-beam panel zones are capacity designed to avoid shear yielding for the expected demands. Additional recommendations for seismic design of SPD-MRF can be found in Tsai et al. (2018).

TEST PROGRAM

Validation of some of the proposed seismic design procedures was achieved through cyclic testing of two, full-scale SPD specimens. Different stiffener details were explored, and the ductile behavior of the SPD was confirmed.

Test Specimens

The two full-scale, 8.53-ft-tall SPD specimens, SPD-2L0T and SPD-2L1T, were identical other than an additional horizontal stiffener for specimen SPD-2L1T [Figure 2(a)]. Each specimen had a 3.94-ft-tall IC and 2.30-ft-tall EJs. The I-sections had overall depth and width of 23.6 in. and 9.84 in., respectively, and 1.18-in.-thick flanges of SN490B (approximately 47-ksi yield stress) steel. The EJ webs were 0.866-in.-thick SN490B steel. The IC webs were 0.315-in.-thick SN400B (approximately 34-ksi yield stress) steel. Properties adopted for the SN400B IC webs included an expected yield stress ratio, R_y, of 1.3 and a strain-hardening factor, ω, of 1.5. SN490B stiffeners included a pair of 0.472-in. × 3.94-in. vertical stiffeners on one side and one 0.984-in. × 3.94-in. horizontal stiffener on the other side of the web for specimen SPD-2L1T. As shown in Figure 2(a), 15.7-in. tall T-shaped stiffeners were added to stiffen the top and bottom end plates used to secure the test specimen to the testing system. Additional details of the test specimens can be found in Tsai et al. (2018).

Test Setup and Loading

NCREE's multiaxial testing system (MATS) was used to apply lateral displacements without rotation or net vertical force, as shown in Figure 2(b). Load cells in the servohydraulic actuators provided forces for determination of shear and bending in the SPD specimens. Displacement transducers [noted as LVDT in Figure 2(b)], tilt meters, and dial gauges were used to determine lateral translations and rotations at top and bottom of the IC and of the SPD. The displacement history followed the cycles of increasing lateral drift as required for cyclic tests for qualification of beam-to-column connections (AISC, 2016).

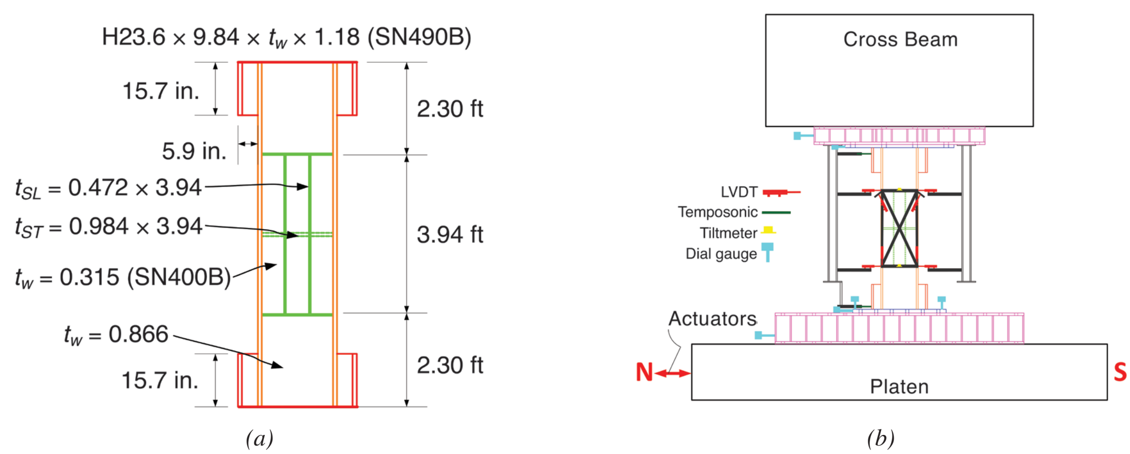

Fig. 2. (a) Details of SPD specimens and (b) test setup.

Experimental Results

The test results validated proposed SPD design procedures. The EJ in both specimens remained elastic throughout the tests. The IC stiffeners effectively delayed shear buckling in the web, and both specimens dissipated energy without apparent strength or stiffness degradation beyond 4% interstory drift (Figure 3). Note that the shear deformations were on the order of 0.11 rad before failure. Specimen SPD-2L0T failed in the first cycle of 5% interstory drift, as can be seen in Figure 3(b), with a fracture that had initiated near a stiffener-to-web weld. Specimen SPD-2L1T failed in the second cycle at 5% interstory drift as shown in Figure 3(a). The slightly larger deformation capacity of SPD-2L1T (a 3% increase in the cumulative plastic deformation capacity) was attributed to the addition of the transverse stiffener. Overall, the shear-deformation response was similar, as shown in Figure 3(c).

NUMERICAL MODELS

Two types of computational models—a shell element model (Abaqus) and a frame element model (PISA3D)—were explored for their effectiveness in predicting the cyclic behavior of the SPD test specimens (Tsai et al., 2018). The Abaqus model, shown in Figures 4(a) and 4(b), was able to represent the cyclic behavior, including strength degradation, quite well, even without simulation of the IC web fractures. The PISA3D model included five beam-column elements, with one representing the IC, two representing EJ without the T-shaped stiffeners, and two representing the portions of the EJ with the T-shaped stiffeners, as shown in Figure 4(c). The beam-column elements were capable of forming shear and/or bending plastic hinges at each end. The IC segment used a two-surface plasticity material model, combining isotropic and kinematic hardening. No fracture or strength degradation was simulated. The PISA3D model was able to reasonably represent the force-deformation response of both specimens up to 4% interstory drift, as shown in Figure 4(d). Additional details of the numerical models can be found in Tsai et al. (2018).

NONLINEAR RESPONSE ANALYSES OF SPD-MRF MODELS

The proposed seismic design procedures were further validated through nonlinear response analyses of a prototype SPD-MRF building. Abaqus and PISA3D models were subjected to cyclic push-pull deformations and simulated ground motions. Some results from the PISA3D models will be presented here.

Prototype Building and SPD-MRF Models

The prototype office building was designed for a location in Chiayi City, Taiwan, with a design peak ground acceleration

(a)

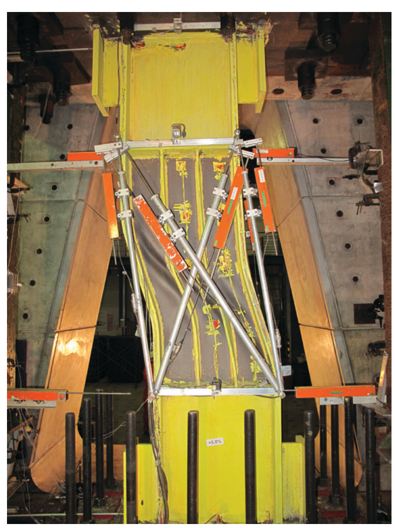

(b)

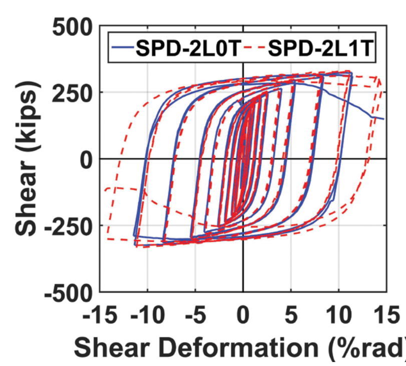

(c)

Fig. 3. (a) Specimen SPD-2L1T at end of test; (b) specimen SPD-2L0T at first cycle of 0.05-rad drift; (c) shear vs. inelastic core rotation.

of 0.33*g*. The six-story building is approximately 177 ft × 108 ft in plan and 68 ft tall, with longitudinal MRF frames and transverse SPD-MRF frames at the perimeter as shown in Figure 5(a). The transverse frames each contain two bays with SPD located at mid-span of 39.4 ft beams as shown in Figure 5(b).

The SPD-MRF were designed with SN400B steel for the IC and SN490B steel for the SPD flanges, EJ webs, and all beams and columns. The 8.53-ft-tall SPDs ranged from approximately 2 ft to 3 ft in depth. IC thicknesses and heights ranged from 0.157 in. to 0.315 in. and 35.4 in. to 70.9 in., respectively. Capacity design procedures were followed to prevent shear or flexural yielding in the boundary beams. Capacity design of SPD-to-beam panel zones resulted in doubler plates at all stories. Additional prototype SPD-MRF design details can be found in Tsai et al. (2018).

The PISA3D model utilized frame elements for all members and centerline dimensions. The prototype building

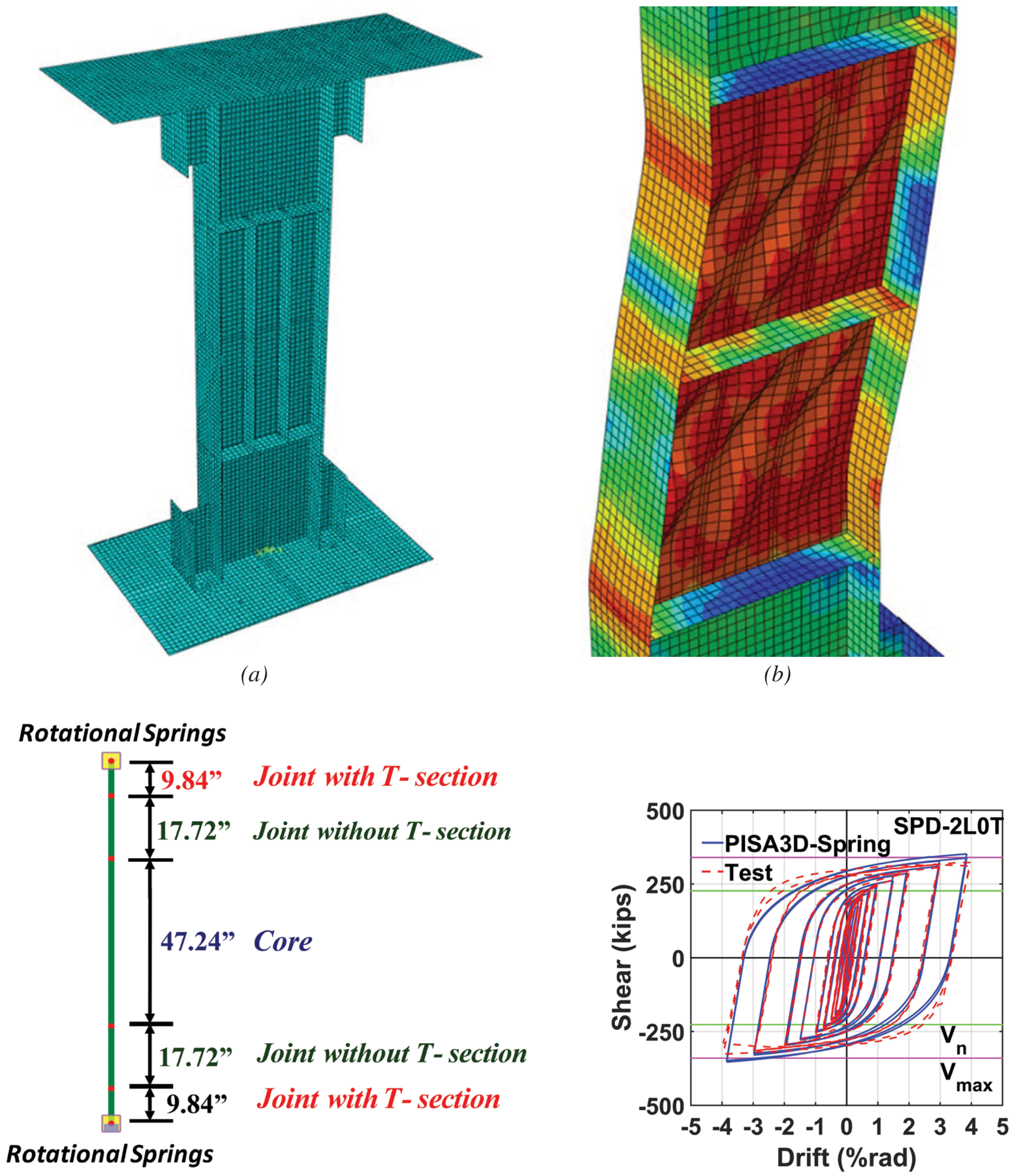

Fig. 4. (a) Abaqus model for specimen SPD-2L1T; (b) deformed shape of Abaqus model; (c) PISA3D model; (d) experimental and PISA3D shear vs. interstory drift for SPD-2L0T.

SPD-to-beam connections did not require T-shaped stiffeners (used to anchor the test specimens to the test set-up), so the SPD models had three elements instead of five. Panel zones were modeled with zero-length joint elements. Rigid offsets were used at beam-column joints. The two-surface plasticity material model was used for the IC elements, and a bilinear kinematic hardening material model was used for all other elements. Additional modeling details, including comparisons with an Abaqus model and cyclic push-pull results, can be found in Tsai et al. (2018).

Seismic Performance of Prototype Building

Nonlinear dynamic time-history analyses were conducted for 240 ground accelerations, evenly distributed across three hazard levels. The ground motions were scaled to spectral accelerations corresponding to the fundamental period of the prototype building in the transverse, SPD-MRF direction. The first 80 ground motions were scaled to the maximum considered earthquake (MCE), the next 80 motions to the design basis earthquake (DBE), and the last 80 to the service level earthquake (SLE).

The primary parameters of interest were the IC rotations, the system overstrength, the maximum roof drift, and the cumulative plastic deformations in the SPD. For IC deformations, the mean, maximum IC rotation was 0.041 rad for the MCE, and the maximum IC rotation never exceeded the 0.11 rad of deformation capacity measured in the SPD tests. Mean plus one standard deviation gave 0.055-rad IC rotation for the MCE. Mean, cumulative plastic deformations (CPD) were also significantly lower than the measured CPD capacities of the SPD. The mean system overstrength was 2.66 for the MCE, 2.46 for the DBE, and 1.34 for the SLE. Mean plus one standard deviation results for maximum roof drift were 1.43%, 1.20% and 0.51% for the MCE, DBE and SLE, respectively, as shown in Figure 6. The design drift limit was satisfied for all DBE ground motions. Analysis results are described in more detail in Tsai et al. (2018).

Additional Design Considerations

The SPD study included more investigation into the T-shaped stiffeners, an equivalent one-element model, and proportioning for stiffness. Analysis of Abaqus models confirmed that the capacity design methods proposed for the EJ are valid for SPD without T-shaped stiffeners. To facilitate use of a simple one-element model that is equivalent to the three-element model, equations were developed for equivalent cross-sectional properties, effective yield stress, and effective post-yield stiffness. A parametric study was also conducted to investigate effects of the IC height ratio and cross-sectional properties on the elastic and post-yield stiffness of the SPD. Methods focused on increasing SPD stiffness without altering the strength of the SPD. Results showed that decreasing the height of the IC and increasing the EJ web thickness were both effective in increasing SPD stiffness.

SUMMARY AND FUTURE WORK

Research has expanded the knowledge base on steel panel dampers beyond behavior, design and detailing of the inelastic core (IC). The work by Tsai et al. (2018) has provided new information on the seismic performance of SPD-MRF, as well as comprehensive guidelines for seismic design of the three-segment SPDs and SPD-MRF. This has been accomplished through testing of two full-scale SPD specimens, design of a six-story prototype SPD-MRF building, and numerical simulations using Abaqus and PISA3D. Seismic design procedures include design of the IC segment and

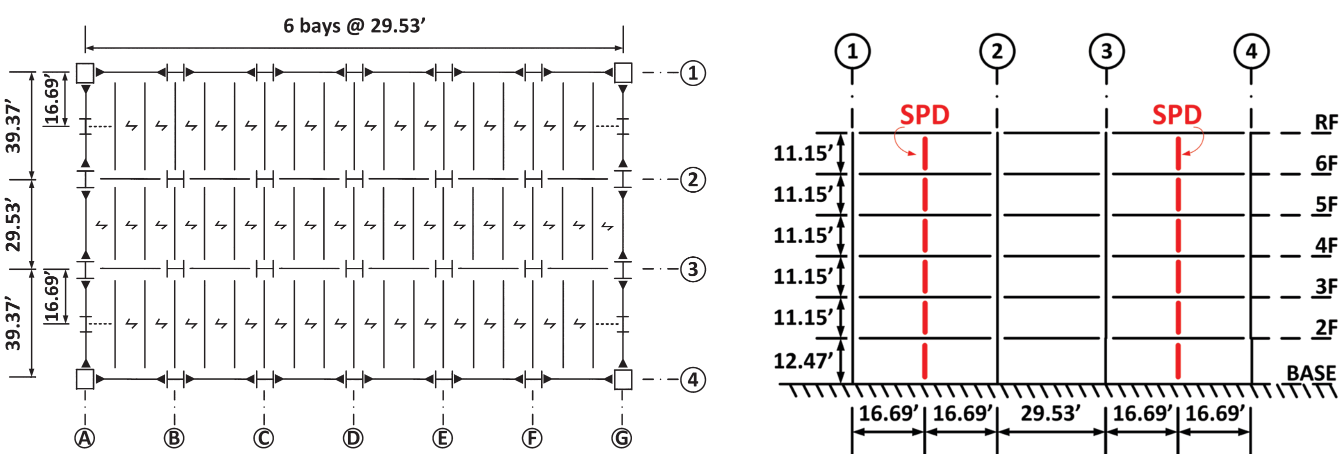

(a) (b)

Fig. 5. (a) Floor framing plan; (b) transverse frame elevation.

capacity design methods (CDM) for the elastic joint (EJ) segments, boundary beams, and the SPD-to-beam panel zones. Additional contributions include a three-segment SPD model, an equivalent one-element model, and guidelines for adjusting properties to achieve higher stiffness without affecting the strength of the SPD.

The decoupled SPD stiffness and strength offers some unique opportunities for design optimization of SPD-MRF. Research is under way on optimization of the stiffness of the SPD and the supporting beams. The studies include investigation into SPD locations with the frame and different options for SPD-MRF configurations.

ACKNOWLEDGMENTS

Special thanks to Dr. Keh-Chyuan Tsai for his many contributions to this article and to Dr. Ching-Yi Tsai, postdoctoral fellow, and former master's students Chung-Hsiang Hsu and Pu-Yuan Chin for creating the figures. Funding for the research was provided by the National Center for Research on Earthquake Engineering (NCREE) and Taiwan's Ministry of Science and Technology, Grant 105-2625-M-002-002. Any opinions, findings, conclusions and recommendations presented in this paper are those of the researchers and do not necessarily reflect the views of the sponsor.

REFERENCES

AISC (2016), *Seismic Provisions for Structural Steel Buildings,* ANSI/AISC 341-16, American Institute of Steel Construction, Chicago, IL.

AISC (2018), *Educator Awards*, American Institute of Steel Construction, www.aisc.org/education/university-programs/educator-awards/#14547, accessed May 9, 2018.

Chen, Z., Ge, H. and Usami, T. (2006), "Hysteretic Model of Stiffened Shear Panel Dampers," *Journal of Structural Engineering,* Vol. 132, No. 3, pp. 478–483. doi: 10.1061/(ASCE)0733-9445(2006)132:3(478).

Lee, J., Kang, H. and Kim, J. (2017), "Seismic Performance of Steel Plate Slit-Friction Dampers," *Journal of Constructional Steel Research,* Vol. 136, pp. 128–139. http://dx.doi.org/10.1016/j.jcsr.2017.05.005.

Lee, J. and Kim, J. (2017), "Development of Box-Shaped Steel Slit Dampers for Seismic Retrofit of Building Structures," *Engineering Structures,* Vol. 150, pp. 934–946. http://dx.doi.org/10.1016/j.engstruct.2017.07.082.

Li, C.H., Wu, C.C., Tsai, K.C., Lin, K.C. and Juang, S.J. (2018), "Fracture Behavior of Electro-Slab Welded Joint in Steel Beam-to-Box Column Connection," *Eleventh U.S. National Conference on Earthquake Engineering,* Los Angeles, CA, June 25–29, 11 pages.

Liu, Y., Aoki, T., Takaku, T. & Fukumoto, Y. (2007), "Cyclic Loading Tests of Shear Panel Damper Made of Low Yield Steel," *Journal of Construction Engineering,* Vol. 53A (in Japanese).

Martinez, C.A. and Curadelli, O. (2017), "Testing and Performance of a New Friction Damper for Seismic Vibration Control," *Journal of Sound and Vibration,* Vol. 399, pp. 60–74. http://dx.doi.org/10.1016/j.jsv.2017.03.022.

NCREE (2018), *AISC/NCREE Special Concentrically Braced Frame Test*. http://exp.ncree.org/scbf/index.html, accessed May 22, 2018.

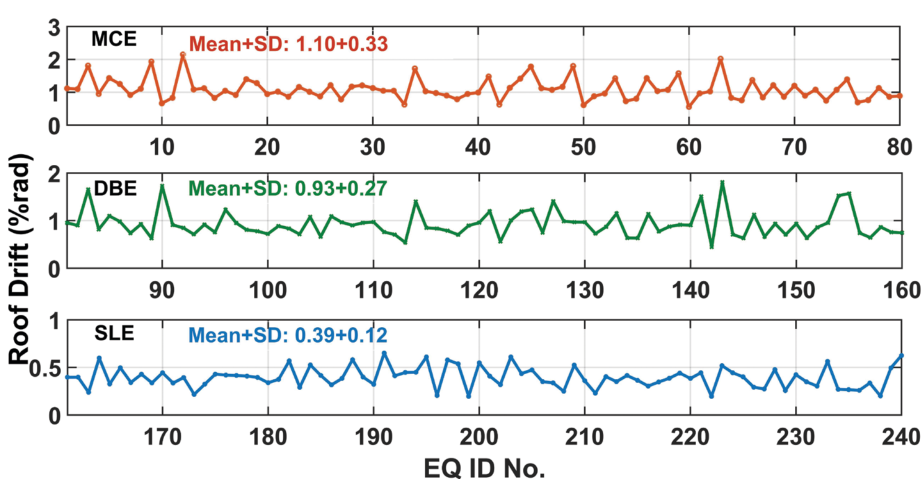

Fig. 6. Nonlinear time-history analysis results for maximum roof drift for each earthquake (EQ) ground motion.

Otani, M., Inai, E., Matsuura, T. and Ito, Y. (2001), "Structural Performance of Shear Panel Dampers Using Low Yield Strength Steel, Parts 1–3," *Abstract Volume of Technical Papers of Annual Meeting, Architectural Institute of Japan* (in Japanese).

Tanaka, K. and Sasaki, Y. (2000), "Hysteretic Performance of Shear Panel Dampers of Ultra Low-Yield Strength Steel for Seismic Response Control of Buildings," *Proceedings of the 12th World Conference on Earthquake Engineering,* WCEE, New Zealand.

Tsai, K.-C., Hsu, C.-H., Li, C.-H. and Chin, P.-Y. (2018), "Experimental and Analytical Investigations of Steel Panel Dampers for Seismic Applications in Steel Moment Frames," *Earthquake Engineering and Structural Dynamics,* Vol. 47, No. 6, pp. 1,367–1,588. http://dx.doi.org/10.1002/eqe.3023.

Tsai, K.-C., Lin, K.-C., Juang, S.-J., Li, C.-H. and Lin, C.-H. (2015), "Research and Practice on Seismic Design of Welded Steel Beam-to-Box Column Moment Connections in Taiwan," *Symposium on Future Development of Seismic Design,* Hong Kong, February 13, 16 pages.

Tsai, K.-C., Wang, H.-Y., Chen, C.-H., Liu, G.-Y. and Wang, K.-J. (2001), "Substructure Pseudo Dynamic Performance of Hybrid Steel Shear Panels," *Steel Structures,* Vol. 1, No. 2, pp. 95–104.

Wang, G., Wang, Y., Yuan, J., Yang, Y. and Wang, D. (2017), "Modeling and Experimental Investigation of a Novel Arc-Surfaced Frictional Damper," *Journal of Sound and Vibration,* Vol. 389, pp. 89–100. http://dx.doi.org/10.1016/j.jsv.2016.11.019.